Experimental determination of crack softening characteristics of normalweight and lightweight concrete

H. A. W. CORNELISSEN, D. A. HORDIJK and
H. W. REINHARDT
Delft University of Technology
Department of Civil Engineering

Summary

For modelling fracture behaviour of concrete various types of deformation controlled uniaxial tests were performed on normalweight and on lightweight concrete. These two types of concrete were compared with respect to their envelope curves, material stiffness and degradation during post-peak cycles, and residual compressive deformation on crack closure. Differences in behaviour were explained on the basis of the properties of the aggregates which result in specific fracture surfaces.

Based on narrow specimens with uniform stress distribution, unique stress deformation curves were determined and the descending branches were modelled. These models were applied to calculate the stress distribution in wide specimens with a sawcut. The total force was in good agreement with the experiment. Probable reasons for the different behaviour of lightweight and normalweight concrete are discussed.

1 Introduction

The tensile properties of concrete are receiving an increasing amount of attention because of several facts such as the interest in punching shear and bending, in the effect of thermal stresses, in durability, but also in fracture mechanics and the application of numerical methods which need a comprehensive description of concrete behaviour.

In the present study, the tensile behaviour of concrete is determined and modelled according to demands from numerical design approaches.

Because of its specific cracking behaviour a normalweight and a lightweight concrete are tested and compared.

2 Theoretical background

Failure of concrete is induced by initiation and propagation of cracks which are governed by the tensile properties of the material. To study this behaviour, information on the stresses in the vicinity of cracks is needed. It is well known that concrete has to be treated as a strain softening material [1, 2]. This implies that in front of a crack tip a softening zone is formed, where the stress distribution $p(t)$ is dependent on deformation and softening characteristics as shown in Fig. 1. The stress distribution in that zone is a function of the deformation and the softening behaviour. According to the approach of Dugdale [3] and Barenblatt [4], the stresses in the softening zone can be regarded as

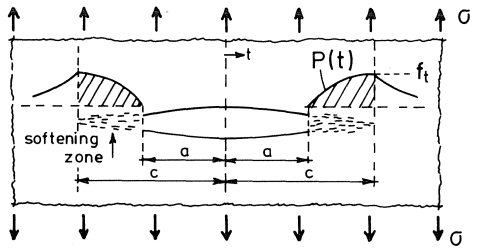

Fig. 1. Crack geometry and stresses in the softening zone.

closing stresses, while in the remaining part of the crack, the crack faces are traction-free.

The stress distribution $p(t)$ depends on the stress-crack opening relation and the crack geometry. If both quantities are known, a fracture criterion for a cracked plate can be established by analytical or numerical means. In order to provide the necessary information which applies to both approaches, stress-crack opening relations should be determined in deformation controlled tensile tests. Moreover, in the case of cyclic loadings the effect of unloading on crack opening has to be determined. Therefore, the experimental programme comprises static and also repeated and alternating loading in the post-peak region of the stress-deformation relation. The tests were carried out on narrow specimens with almost uniform stress distribution.

To check the validity of the theoretical assumption wide specimens were loaded uniaxially. The deformation distribution around saw-cuts, together with the previously determined stress-crack opening relation, should enable the stress-elongation relation of these wide specimens to be predicted.

3 Experiments

3.1 *Types of concrete and specimens*

The experimental programme consisted of tests on a normalweight and on a lightweight concrete (abbreviated as NC and LC respectively). For NC river gravel with maximum grain size of 8 mm was used, and a sintered expanded clay (4–8) for LC. The lightweight aggregate was manufactured by Compagnie des Ciments Belges and specified as ISOL S 4–8, with bulk density of 1260 kg/m^3. Details of mix composition and mechanical properties are listed in Table 1.

The cubes (150 mm) for the standard compressive and splitting tests were stored in water until testing at an age of 28 days. The direct tensile strength and Young's modulus, however, were determined in deformation controlled tests on specimens (see further), which were first cured in water for 14 days and subsequently in the laboratory (20 °C, 60% RH) until testing at 45–55 days after casting. The relatively low direct tensile strength of LC is probably due to the effect of shrinkage stresses which are more pronounced in the case of LC. This feature has also been reported in [5].

Table 1. Properties of the types of concrete tested.

mix proportions	normalweight (kg/m^3)	lightweight (kg/m^3)
Portland cement	375	400
sand 0-2 mm	905	598
sand 2-4 mm	363	-
gravel 4-8 mm	540	-
lightweight aggregate 4-8 mm*	-	732
water	187.5	129
superplasticizer	-	6
density	2370	1865
mechanical properties	**(N/mm^2)**	**(N/mm^2)**
compressive strength	47.1 (6.0%)**	48.6 (6.0%)
splitting strength	3.20 (9.4%)	3.66 (8.3%)
direct tensile strength	3.20 (9.7%)	2.43 (8.6%)
Young's modulus (tension)	39270 (8.5%)	22420 (6.1%)

* incl. 17% by weight absorbed water.
** coefficiënt of variation.

The specimens for the deformation controlled tensile tests were cut from 50 mm thick panels which were cast in the vertical position. Two specimen geometries were applied: narrow ones 250 mm × 60 mm × 50 mm, where a saw-cut (5 mm width) reduced the cross-section to 50 mm × 50 mm; wide ones 250 mm (length) × 220 mm × 50 mm with an effective cross-section of 180 × 50 mm as also created by saw-cuts. The narrow specimens were used to determine stress-crack opening relations, while the wide specimens provided information on the softening zone.

3.2 *Testing equipment*

Tests were carried out on a closed-loop electro-hydraulic loading machine with a capacity of 100 kN in tension and in compression (see Fig. 2). For the deformation controlled tests, the averaged signal from two LVDTs mounted on the specimens was compared with the signal from a specially designed ramp generator. The deformation rate for the narrow specimens was 0.08 μm/s. In cyclic tests up to the envelope curve the direction of deformation was reversed either along the envelope curve when the loading dropped by a certain amount (120 N), or at a preset lower force level which could be tensile or compressive.

The specimens were glued between steel platens. The lower platen was fixed, whereas the upper was connected to the actuator. Bending of the specimen was reduced by a guiding system provided with ball bushings of the upper platen. The (low) friction of this system was taken into account in the analysis of the loading readings.

Deformation measurements of the specimens were obtained with LVDTs, with electromechanical gauges (35 mm base) and occasionally with 20 mm strain gauges. These instruments were attached over the reduced cross-section. The signals from them were

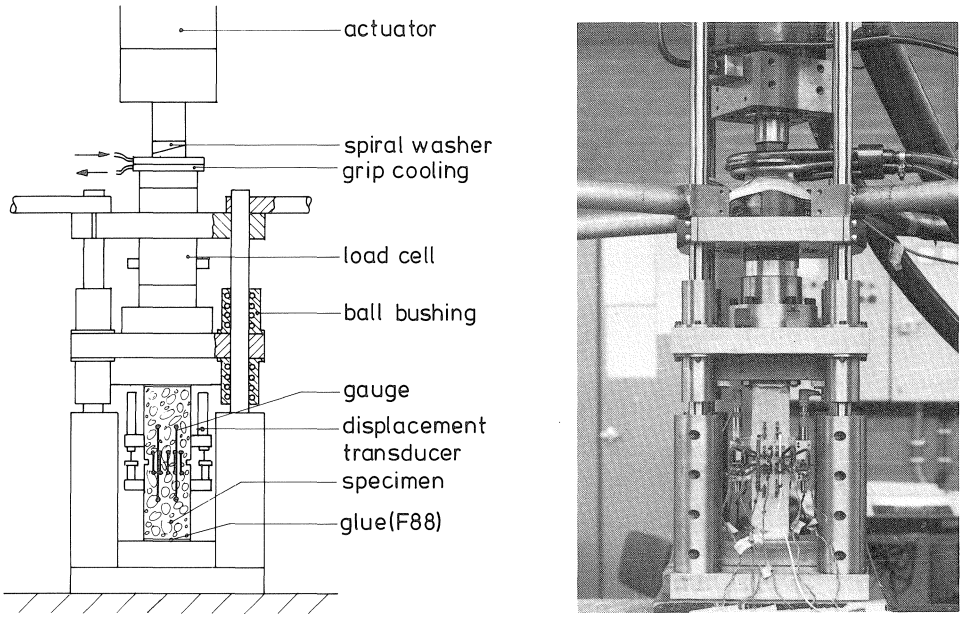

Fig. 2. View of the testing equipment.

transmitted to a microcomputer which also controlled the sampling rate, namely, six per second, after adjustable time intervals. The results were punched on paper tape and processed with the main laboratory computer.

3.3 *Types of test*

The main object of the experimental programme was to provide stress-crack opening relations. In order to study the effect of cyclic loading on this relation as well, basically four types of uniaxial test were performed, denoted by type a, b, c and d in Fig. 3. Type a refers to deformation controlled tensile tests; in types b, c and d, post-peak cycles were applied between a tensile stress, a low compressive stress or a higher compressive stress and the envelope curve respectively. It can be seen that in the case of post-peak cycles the lower level was 10%, -15% or -100% of the tensile strength.

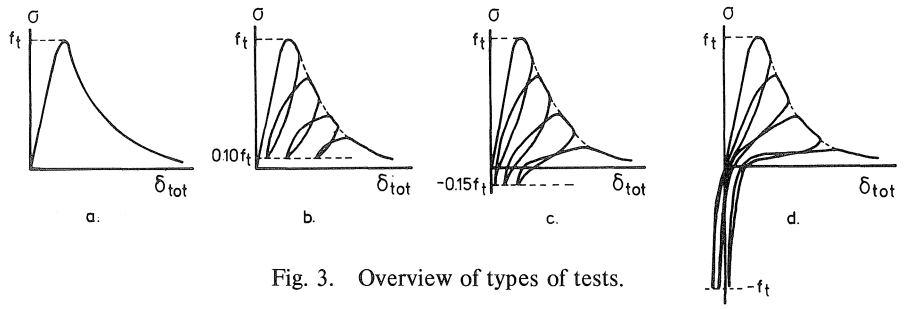

Fig. 3. Overview of types of tests.

4 Envelope curves

Stress-deformation relations were obtained from narrow specimens. In Fig. 4 a typical result is shown of a post-peak cyclic test on LC. The stress is calculated as the force divided by the area of the cross-section between the saw-cuts, while the deformation is the mean value of five readings on the front as well as on the rear face of the specimen. In the diagram on the right the strain distribution across the specimens is also given. Here the corresponding readings at front and rear were averaged. According to the starting points, the diagram shows uniformly distributed strains at all loading steps except at those where cracking obviously starts on one side of the specimen.

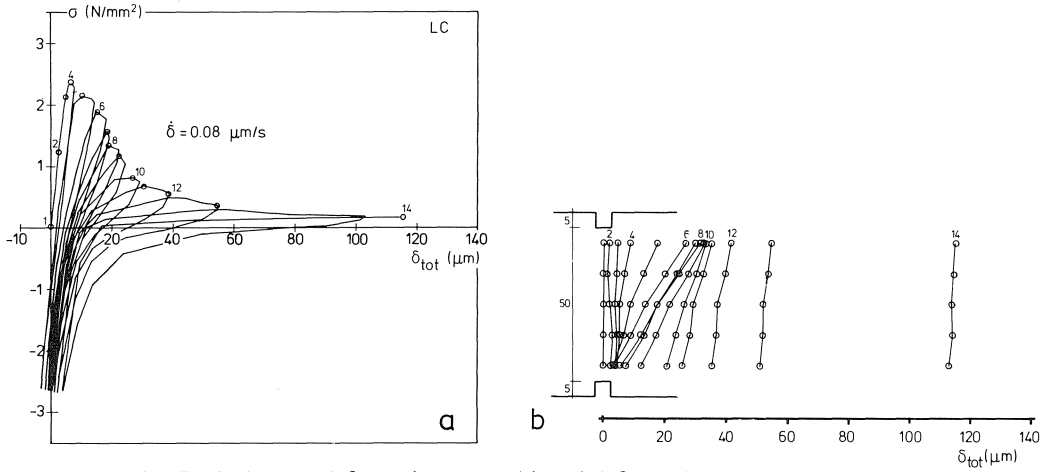

Fig. 4. Typical stress deformation curve (a) and deformation distribution for LC (b).

In the case of post-peak cyclic tests, the corresponding relation between deformation and ultimate stress on the descending branch is normally called the envelope curve. These envelope curves are found practically to coincide with the static test results, as can be seen in Fig. 5 for NC and for LC too. The lines in this diagram are averages of three individual tests of the types a to d (defined in Fig. 3). It can be concluded that for a

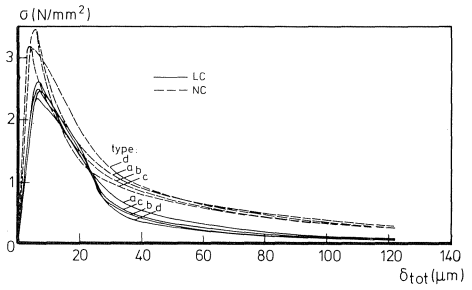

Fig. 5. Envelope curves for NC and LC from testing types a to d (see Fig. 3).

given concrete there exists a unique relation between crack opening and ultimate stress, which is not affected by stress or strain history.

As appears from the diagram the tensile strength of LC is smaller than that of NC. Young's modulus for LC is about 0.6 times that for NC. The strain at maximum stress (δ_{tot}/gauge length) amounts to 135 microstrain for NC and 180 microstrain for LC.

The lines also indicate that at deformations of more than about 25 μm, load transfer for LC is less than for NC, which is presumably due to the crack surface, which in the case of LC is smoother because the cracks pass through the aggregate particles, whereas in NC the cracks propagate along grain surfaces, which allows sliding friction.

The stress-deformation relations in Fig. 5 were transformed into stress-crack opening relations, in which the crack opening δ is defined as the total deformation (δ_{tot}) minus an elastic part and a part which takes account of non-elastic effects during unloading of the material adjacent to the crack faces. These parts are represented by an unloading line from the top of the σ–δ_{tot} curve parallel to the first loading branch.

The following mathematical model is found to fit the data points for both types of concrete quite satisfactorily:

$$\sigma/f_t = f(\delta) - (\delta/\delta_0) f(\delta = \delta_0) \tag{1}$$

in which:

$$f(\delta) = (1 + (C_1\delta/\delta_0)^3) \exp(-C_2\delta/\delta_0)$$

By means of regression analysis, optimum values were estimated for δ_0, C_1 and C_2. The results are shown in Fig. 6. The crack opening at which stress no longer can be transferred (δ_0) was estimated as 140 μm for LC and 160 μm for NC, where sliding friction is more important, as already stated.

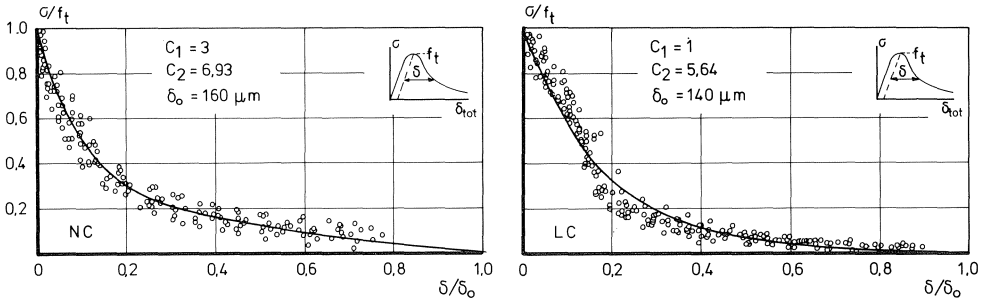

Fig. 6. Stress-crack opening relations for NC and LC according to the model of equation (1).

The standard deviations or the error in the σ/f_t direction prove to be 0.052 for NC and 0.063 for LC.

The shape of the envelope curve represented by equation (1) was satisfactory, as was ascertained in numerical sensitivity studies for the calculation of the fracture behaviour of notched beams [6].

The area under the stress-crack opening relation is a measure for the fracture energy, usually called G_f. Based on equation (1) with mean values for f_t, $G_f = 100$ N/m for NC and 61 N/m for LC. The characteristic length according to Petersson [7]: $l_{ch} = EG_f/f_t^2$ is 380 mm for NC and 230 mm for LC respectively.

5 Post-peak cyclic behaviour

For modelling the post-peak behaviour it is necessary also to have information on the relations between stress and deformation during unloading and reloading. For this reason test results obtained from narrow specimens were evaluated. Characteristics will be discussed with reference to the decline in stiffness, the increase in damage due to load cycles (which is indicated by the stress drop on the envelope curve), and the residual strain at the maximum of the applied compressive stress.

5.1 *Stiffness degradation*

For the analysis of stiffness degradation of the specimens during cyclic loading, a distinction was made between the unloading and the reloading behaviour. The stiffness was defined as the slope of the linear part in the corresponding branch. However, in the case of test type b, which shows continuous non-linear branches, the stiffness was estimated according to a straight line through the minimum of the cycle and the appropriate point on the envelope curve. This is clarified in Fig. 7a and 7b for the unloading and (re-)loading branches respectively. It is also shown that stiffness C is referred to the initial stiffness C_0. This relative stiffness is plotted versus crack opening δ at the start of unloading in each cycle. The lines presented are averages of three individual results.

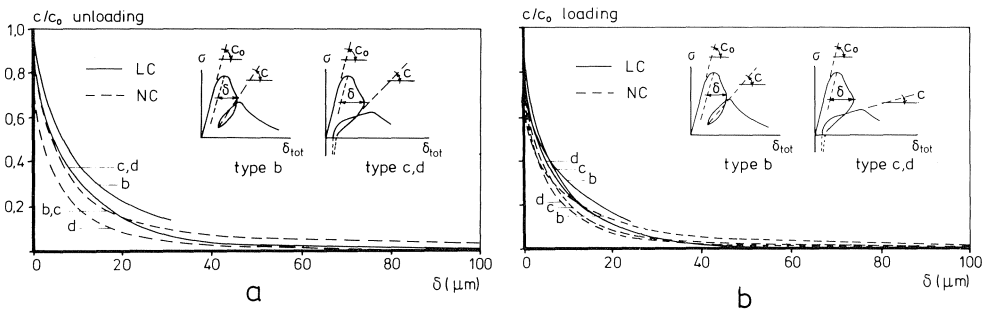

Fig. 7. Stiffness decline during post-peak unloading (a) and (re-)loading (b).

- unloading stiffness

Diagram 7a for the unloading stiffness shows a steep decrease in the first cycles. At a crack opening of 10 μm the stiffness is only about 40% of the original value for LC and 25% in the case of NC. The relatively rapid degradation of NC emerged also from the envelope curves in Fig. 5.

For both types of concrete there is no significant effect of the type of test, which is in agreement with the assumption that the relation between stress and crack opening is not affected by preceding behaviour.

- reloading stiffness

The development of the relative stiffness of the (re-)loading path is expressed by Fig. 7b. Here the decrease in stiffness is even more pronounced than for the unloading path, as follows from the comparison of C/C_0 at a crack opening of 10 μm for both paths. For reloading, the corresponding values are 30% for LC and 20% for NC. This marked decrease is probably due to additional crack propagation in the preceding unloading parts of the cycles.

For NC as well as for LC a slower decrease in reloading stiffness can be observed in the case of type b tests, indicating that preceding unloading in tension is less detrimental than in compression. However, more experimental data is needed to support these findings.

5.2 *Stress drop*

The stress drop on the envelope curve as affected by load cycles also reflects the crack opening behaviour of the material and should therefore be included in correct material models.

Let σ_{eu} be the stress at which a given unloading cycle leaves the envelope curve. The decrease in stress on returning to this envelope curve is called the stress drop, $\Delta\sigma$. In Fig. 8 the relative stress drop is plotted against crack opening for NC and LC. For each type of test, data points from three specimens are indicated. By means of linear regression, straight lines were fitted to these points. As can be seen, because of the scatter, only trends can be discussed.

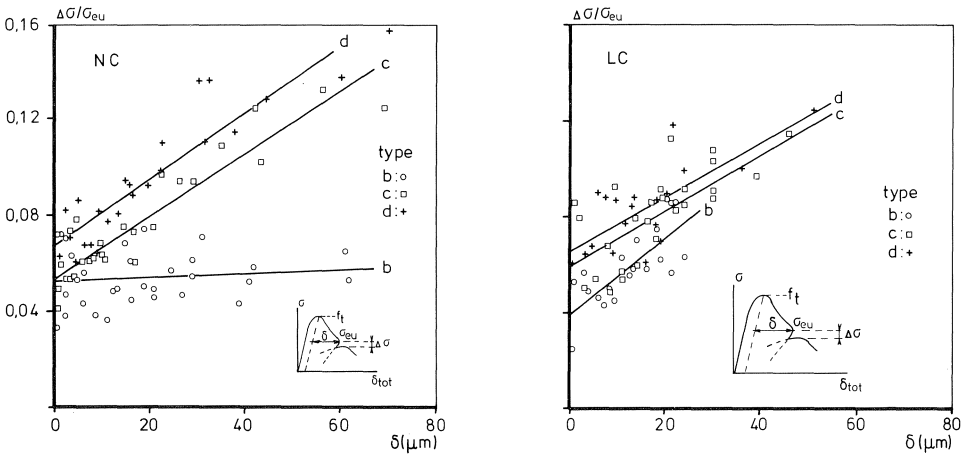

Fig. 8. Stress drop on the envelope curve after post-peak loading cycles.

For NC as well as for LC the development of stress drop is approximately similar for types c and d (see Fig. 3 for explanation), showing an increase in relative stress drop from about 6% up to about 14% at a crack opening of 60 μm. In the case of test type b however, the relative stress drop for LC also increases, while NC shows an almost constant value, indicating a decreasing absolute $\Delta\sigma$. This can be explained by the fact that during a small amount of unloading in tension the crack surfaces may fit rather well for NC, resulting in minor damage, whereas in the case of LC because of its smooth crack surfaces, small transverse displacements are possible, which prevent crack closure on unloading and consequently give rise to extra damage.

The relative stress drop is more for types d and c than for type b for NC, and to a lesser extent for LC. This again shows the detrimental effect of compressive unloading (types c, d) on the tensile properties.

5.3 *Residual compressive deformation*

For test types d, the residual deformation in compression was measured. This deformation, which was reached after unloading from a certain crack opening on the envelope curve, was referred to the compressive deformation which follows from the stiffness of the first loading branch (see Fig. 9).

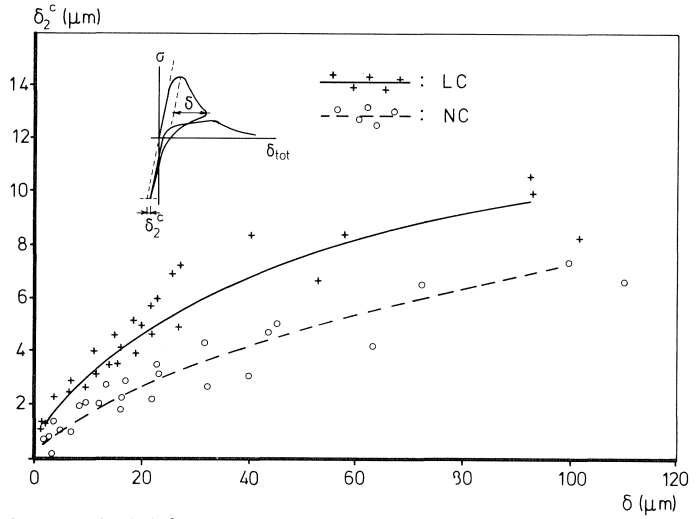

Fig. 9. Residual deformation (δ_2^c) after post-peak unloading in compression.

A gradual increase in residual deformation can be observed up to about 7 μm for NC and up to 10 μm for LC at $\delta = 100\mu m$. The higher values for LC may be due to the mismatch of fracture surfaces accompanied by the formation of small crushed particles in the crack as pointed out before.

6 Stress distribution in a wide cracked plate

In deformation controlled tests on wide specimens the deformation distribution over the cross-section between the saw-cuts was measured in various stages of the experiment (see Fig. 10).

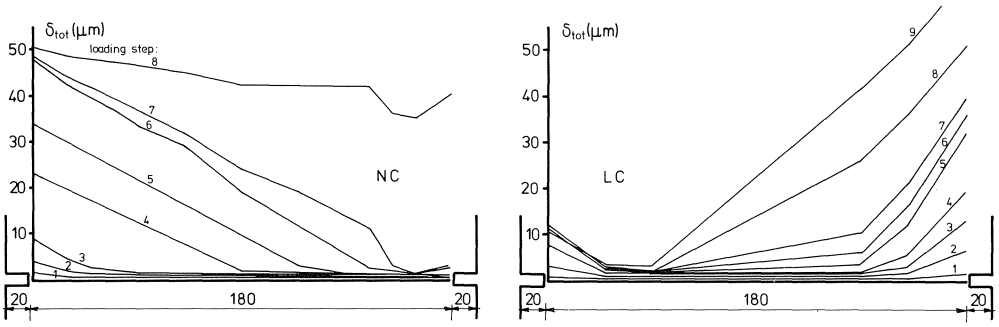

Fig. 10. Deformation distribution of wide NC and LC specimens.

Because bending could not be excluded completely, both diagrams show symmetric deformation distributions during the first loading steps, but eccentric deformation occurs later on. This, however, does not affect the aim of these tests, which was to predict the overall stress-deformation behaviour of a wide cracked plate by making use of local deformation and general stress-crack opening relations.

In order to minimize the error, most data should be taken from the actual specimen, i.e. Young's modulus and tensile strength. If taken from average values of other test series, scatter would already enter the calculation. Therefore, Young's modulus was determined from the strain distribution in the pre-peak state and the condition of equilibrium, i.e. $\int E\varepsilon dx =$ total external force. Using this Young's modulus, the total external load at subsequent loading stages was calculated. At a certain load, predicted and measured total force were not in agreement. By iteration and use of eq. (1) for the descending branch the tensile strength could then be calculated. Both quantities (E and f_t) fell within the scatter band of the results for narrow specimens.

Based on the relations obtained, stress distributions were deduced from the experimentally determined deformation distribution in Fig. 10. Some typical examples are presented in Fig. 11. It is clearly demonstrated that the softening zone spreads from the edge over the whole cross-section for increasing deformations.

The total force calculated from the stress distribution curves was divided by the original cross-sectional area and plotted against the mean deformation (35 mm base) in Fig. 12. The measured force divided by the original cross-sectional area is also represented in these diagrams, which show good agreement, confirming the applicability of the proposed method.

On comparing the loading branches of the σ–δ_{tot} curves in Fig. 12 there is seen to be

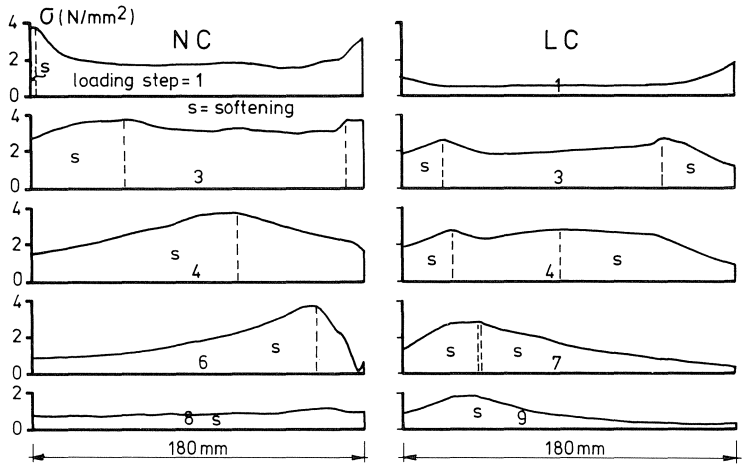

Fig. 11. Calculated stress distribution of wide specimens.

marked difference between the two types of concrete. NC shows a linear behaviour up to load step 2, which is 90% of the maximum load. From step 2 to 3 the stiffness is a little less. After the top has been reached the stress decreases rather rapidly to about 60% at step 5. In the case of LC, linear behaviour can be observed up to 65% of the maximum load, then a gradual non-linear increase of deformation occurs until the top, and thereafter a progressive decrease in stress which is less than for NC. This different behaviour may be explained by the stress-deformation lines of Fig. 5, which shows a larger strain at maximum stress for LC than for NC. This means that for the stress distribution for a given strain concentration near the saw-cut NC reaches the top at smaller strains than LC does and that the softening zone of NC contributes less to the load than LC does. Or, expressed in another way, LC reaches the maximum stress at the saw-cut at a smaller load than NC, but contributes longer to the total load because of its more ductile behaviour. This means that between step 3 and 4 for NC the softening zone expands rapidly and already reaches the middle of the specimen, whereas LC exhibits a rather pronounced strain concentration up to step 7. Presumably the rapid stress release of NC assists the softening expansion also by dynamic effects.

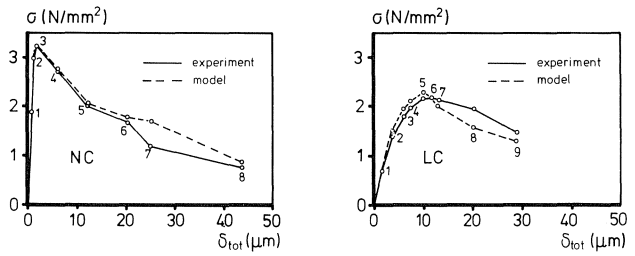

Fig. 12. σ–δ_{tot} relations for NC and LC as measured and as predicted for wide specimens.

7 Conclusions

1. The tensile envelope curves for normal as well as for lighweight concrete are not significantly affected by cyclic loading.
2. Because of the uniform stress distribution in the narrow specimens, the models for the descending branch based on these specimens can be regarded as material properties.
3. Damage in the unloading branch probably affects the stiffness decline in the subsequent loading branch. For crack openings smaller than about 25 μm, LC shows less decline than NC as indicated by reloading and unloading post-peak stiffness.
4. Damage indicated by relative stress drop along the envelope curve is affected by the lower level of the loading cycle. Because of extra damage induced by mismatch of fracture surfaces, the effect is less pronounced for LC.
5. Based on models derived from narrow specimens, stress distribution in wide specimens could be calculated.
6. The softening zone in the vicinity of a crack spreads faster in normal weight concrete than in lightweight concrete, once the tensile strength is reached.

8 Acknowledgements

These investigations were partly supported by the Netherlands Foundation for the Technical Sciences (STW), future Technical Science Branch Division of the Netherlands Organization for the Advancement of Pure Research (ZWO).

The authors wish to express their gratitude to Mr. G. Timmers for his valuable assistance.

9 References

1. H. W. Reinhardt, Fracture mechanics of an elastic softening material like concrete, Heron, Vol. 29, No. 2, 1984, 42 pp.
2. A. Hillerborg, Analysis of fracture by means of the fictitious crack model particularly for fibre reinforced concrete, Int. Journal of Cement Composites, 2, 1980, pp. 177–184.
3. D. S. Dugdale, Yielding of steel sheets containing slits, Journal of Mechanics and Physics of Solids, 8, 1960, pp. 100–104.
4. G. I. Barenblatt, The mathematical theory of equilibrium cracks in brittle fracture, Advances in Applied Mechanics, 7, 1962, pp. 55–129.
5. B. Fouré, Note sure la chute de résistance a la traction du béton léger consécutive à l'arrêt de la cure humide. Ann. de l'Inst. Techn. du Bâtiment et des Travaux Publics, No. 432, 1985, pp. 1–15.
6. J. G. Rots, Strain-softening analysis of concrete fracture specimens. Preprints Rilem Int. Conf. on Fracture Mechanics of Concrete, Lausanne, Vol. 1, 1985, pp. 115–126.
7. P. E. Petersson, Fracture energy of concrete: Method of determination, Cement and Concrete Research, Vol. 10, 1980, pp. 79–89.